REGULAR ARTICLE

blood advances

Packaging of supplemented urokinase into alpha granules of in vitro–grown megakaryocytes for targeted nascent clot lysis

Mortimer Poncz,[1,2,*] Sergei V. Zaitsev,[1,*] Hyunsook Ahn,[1,*] M. Anna Kowalska,[1,3] Khalil Bdeir,[4] Konstantin V. Dergilev,[5] Lacramioara Ivanciu,[1,2] Rodney M. Camire,[1,2] Douglas B. Cines,[4] and Victoria Stepanova[4]

[1]Department of Pediatrics, Children's Hospital of Philadelphia, Philadelphia, PA; [2]Department of Pediatrics, University of Pennsylvania, Perelman School of Medicine, Philadelphia, PA; [3]Institute of Medical Biology, Polish Academy of Sciences, Lodz, Poland; [4]Department of Pathology and Laboratory Medicine, University of Pennsylvania, Perelman School of Medicine, Philadelphia, PA; and [5]Institute of Experimental Cardiology, National Medical Research Center of Cardiology named after Academician E.I. Chazov, Moscow, Russia

Key Points

- Unlike platelets, in vitro–grown megakaryocytes can take up and store exogenous uPA into their α-granules.
- uPA uptake involves LRP1 and αIIβ3 receptors and is functionally available upon platelet activation.

Fibrinolytics delivered into the general circulation lack selectivity for nascent thrombi, reducing efficacy and increasing the risk of bleeding. Urokinase-type plasminogen activator (uPA) transgenically expressed within murine platelets provided targeted thromboprophylaxis without causing bleeding but is not clinically feasible. Recent advances in generating megakaryocytes prompted us to develop a potentially clinically relevant means to produce "antithrombotic" platelets from $CD34^+$ hematopoietic stem cell–derived in vitro–grown megakaryocytes. $CD34^+$ megakaryocytes internalize and store in alpha granules (α-granules) single-chain uPA (scuPA) and a plasmin-resistant thrombin-activatable variant (uPAT). Both uPAs colocalized with internalized factor V (FV), fibrinogen and plasminogen, low-density lipoprotein receptor–related protein 1 (LRP1), and interferon-induced transmembrane protein 3, but not with endogenous von Willebrand factor (VWF). Endocytosis of uPA by $CD34^+$ megakaryocytes was mediated, in part, via LRP1 and αIIbβ3. scuPA-containing megakaryocytes degraded endocytosed intragranular FV but not endogenous VWF in the presence of internalized plasminogen, whereas uPAT-megakaryocytes did not significantly degrade either protein. We used a carotid artery injury model in nonobese diabetic-severe combined immunodeficiency IL2rγnull (NSG) mice homozygous for VWF^{R1326H} (a mutation switching binding VWF specificity from mouse to human glycoprotein Ibα) to test whether platelets derived from scuPA- or uPAT-megakaryocytes would prevent thrombus formation. NSG/VWF^{R1326H} mice exhibited a lower thrombotic burden after carotid artery injury compared with NSG mice unless infused with human platelets or megakaryocytes, whereas intravenous injection of uPA-megakaryocytes generated sufficient uPA-containing human platelets to lyse nascent thrombi. These studies describe the use of in vitro–generated megakaryocytes as a potential platform for delivering uPA or other ectopic proteins within platelet α-granules to sites of vascular injury.

Submitted 2 February 2024; accepted 18 May 2024; prepublished online on *Blood Advances* First Edition 28 May 2024. https://doi.org/10.1182/bloodadvances.2024012835.

*M.P., S.V.Z., and H.A. contributed equally to this study.

Data are available on request from the authors, Victoria Stepanova (vstepano@pennmedicine.upenn.edu) or Mortimer Poncz (poncz@chop.edu).

The full-text version of this article contains a data supplement.

Introduction

There is an unmet need for safe and effective therapeutics to treat or prevent thromboembolism in settings such as postextensive surgery or trauma. Yet, the risk of bleeding often delays the introduction of anticoagulation in the immediate postevent timeframe. In these settings, there is a need for therapies that distinguish preexisting hemostatic clots, leaving them intact, while targeting for fibrinolysis nascent, potentially occlusive, thrombi.

Fibrinolytic agents, such as the plasminogen (PLG) activators (PA), tissue-type PA (tPA), and urokinase PA (uPA) are effective at lysing thrombi[1-3] but permeate preexisting hemostatic fibrin[4] and can degrade circulating fibrinogen.[5] Both PAs have short half-lives, necessitating continuous intravenous infusions for prophylaxis,[6] and have vasoactive and neurotoxic side effects after a stroke (reviewed in Medcalf[7]). Therefore, the clinical use of fibrinolytic agents has been limited primarily to the management of a subset of patients with acute ischemic stroke or life- or limb-threatening thromboembolism.[8-10]

To address these limitations, we found that PAs linked to red blood cells or platelets (PLTs) provide protracted and safe thromboprophylaxis in several animal models.[11,12] However, red blood cells are not rapidly and selectively recruited to sites of incipient arterial thrombus formation,[13] and linking the PAs to the surface of the PLTs can lead to thrombocytopenia and bleeding in mice and nonhuman primate models (M. Poncz, S. Zaitsev, and D. Myers, University of Michigan, unpublished observations, September 2015).

As an alternative approach, we ectopically expressed single-chain (sc) murine (m) uPA in megakaryocytes (MKs)/PLTs of transgenic mice. The m-scuPA was stored in PLT alpha granules (α-granules) without causing systemic fibrinolysis. The transgenic mice had a mild bleeding diathesis during parturition,[14] ameliorated by tranexamic acid, which inhibits plasmin and uPA activity.[15] These mice simulated human Quebec platelet disorder (QPD), which is caused by a duplication of the uPA gene (*PLAU*), also characterized by storage of uPA in PLT α-granules,[16-19] absence of systemic fibrinolysis, and a mild bleeding diathesis mitigated by tranexamic acid.[14] We have previously shown that infusion of the uPA-containing PLTs (uPA-PLTs) into wild-type mice prevented nascent thrombus growth in a microemboli infusion model.[14] This raises the possibility that delivering uPA packaged within PLT α-granules inverts PLT function from prothrombotic to fibrinolytic and does so in a manner that does not lyse mature clots that are no longer recruiting PLTs.[14]

Recent advances in the generation of PLTs from in vitro–grown MKs have been made, especially beginning with induced pluripotent stem cells.[20-22] A recent paper describing the infusion of PLTs generated from induced pluripotent stem cells into a patient as a PLT transfusion had been described.[23] We wondered whether in vitro–grown MKs can endocytose uPA from the media as the MKs are grown in defined media and thus lack the normal array of endocytosed proteins. Prior studies have shown that these in vitro–grown MKs can endocytose added fibrinogen and factor V (FV).[24] Here, we show that scuPA or a thrombin- but not plasmin-activatable uPA (uPAT)[11] added to the media were readily endocytosed by maturing MKs. We define receptors involved in their uptake and the interaction of these uPAs with other endocytosed and with endogenous α-granular proteins. Using an in vivo murine carotid artery photochemical injury model, we show that the uPAs studied can effectively prevent thrombus development. We discuss potential uses of this approach for targeted thromboprophylactic fibrinolysis and the application of this strategy for delivering other ectopic therapeutics via PLTs.

Materials and methods

Supplemental methods

Please see supplemental Methods for additional methods, including western blotting (WB) and agonist activation studies, and a description of reagents and antibodies.

Generation of uPA-containing MKs (uPA-MKs)

Granulocyte colony-stimulating factor–mobilized human $CD34^+$ hematopoietic progenitor cells, purchased from the Fred Hutchinson Cancer Research Center Hematopoietic Cell Processing and Repository Core, were differentiated into MKs ($CD34^+$ MKs), as we have previously described.[25] Day 10 or 11 $CD34^+$ MKs were incubated for various times in complete growth medium containing various combinations of the following fluorophore-conjugated proteins: scuPA, uPAT, noncleavable PLG (ncPLG),[26] recombinant receptor-associated protein linked to human immunoglobulin G Fc fragment (FcRAP),[27] and FV. The $CD34^+$ MKs were washed once with phosphate-buffered saline and immobilized on microscopic slides using Shandon CytoSpin III Cytocentrifuge with the M964-20FW-CytoSep for 15 minutes. Please, see details of immunofluorescent staining and confocal laser-scanning microscopy in the supplemental Methods.

Flow cytometry studies of protein uptake

$CD34^+$ MKs differentiated for 10 to 11 days were incubated in complete growth medium containing a combination of the following fluorophore-conjugated proteins: scuPA, uPAT, and FV. Unlabeled FcRAP[27] or the blocking αIIbβ3 monoclonal antibody ReoPro[28,29] were used as lipoprotein receptor–related protein 1 (LRP1) and αIIbβ3 antagonists, respectively. The uptake of endocytosed fluorescent proteins was analyzed in $CD42b^+$ population using a CytoFlex S flow cytometer (Beckman). Please see supplemental Methods for more details.

In vivo murine studies

Nonobese diabetic-severe combined immunodeficiency IL2rγnull (NSG) mice were originally purchased from The Jackson Laboratory. The transgenic NSG/VWF^{R1326H} mice, homozygous for a CRISPR/CRISPR-associated protein 9 mutation in murine von Willebrand factor (VWF), has been described previously.[30,31] Before infusion, MKs were or were not preloaded with recombinant scuPA or uPAT as follows: day-10 $CD34^+$ MKs were left intact or incubated with recombinant scuPA or uPAT (600 nM each) for 24 hours in the culture media. The cells were washed and resuspended in phosphate-buffered saline at a concentration of 3×10^7 $CD34^+$ MKs per mL. Please see supplemental Methods for details of the thrombosis model.

Measurement of endocytosed scuPA in MK lysates

scuPA protein concentration in the untreated and scuPA-treated MK lysates was measured using the huPA Quantikine enzyme-linked immunosorbent assay kit (R&D Systems) per manufacturer. Please see supplemental Methods for details.

Statistical analysis

Means ± standard deviation are shown. For data obtained by flow cytometry, differences were analyzed by ordinary 1-way analysis of variance. For in vivo studies, differences in carotid blood flow in the photochemical carotid injury studies were analyzed by ordinary 1-way analysis of variance using GraphPad Prism 5. For all studies, differences were considered significant with a P value of $< .05$ compared with the indicated control.

Institutional approval of studies

Approval was obtained from the institutional internal review board for the volunteer blood samples. These studies were conducted in accordance with the Declaration of Helsinki. Murine studies had institutional animal care and use committee approval. Euthanasia was performed as approved by the Panel on Euthanasia of the American Veterinary Medical Association.

Results

Endocytosis of uPA by in vitro–grown MKs

We, and others, have shown that in vitro–generated MKs differentiated in defined media can endocytose fibrinogen, FVIII, and FV until the late stages of differentiation[24,32,33]; however, given the lack of these proteins in the growth media, these proteins would be absent from the α-granules. Perhaps if exogenous uPA, not normally found in PLTs,[14] were added to the media, the MKs would endocytose and store uPA in their α-granules, and be useful to generate uPA-PLTs for targeted thrombolysis. We, therefore, added to the media scuPA. This uPA contains the N-terminal uPA-receptor (uPAR)-binding growth factor-like domain, a Kringle domain, and a C-terminal proprotease domain (Figure 1A, top). scuPA is dependent on uPAR as well as LRP1 for uptake into cells.[34] We also studied a low–molecular weight variant we developed,[11] designated uPAT, which lacks the 2 N-terminal domains (Figure 1A, bottom), making it incapable of binding to uPAR. uPAT is activated by thrombin, for

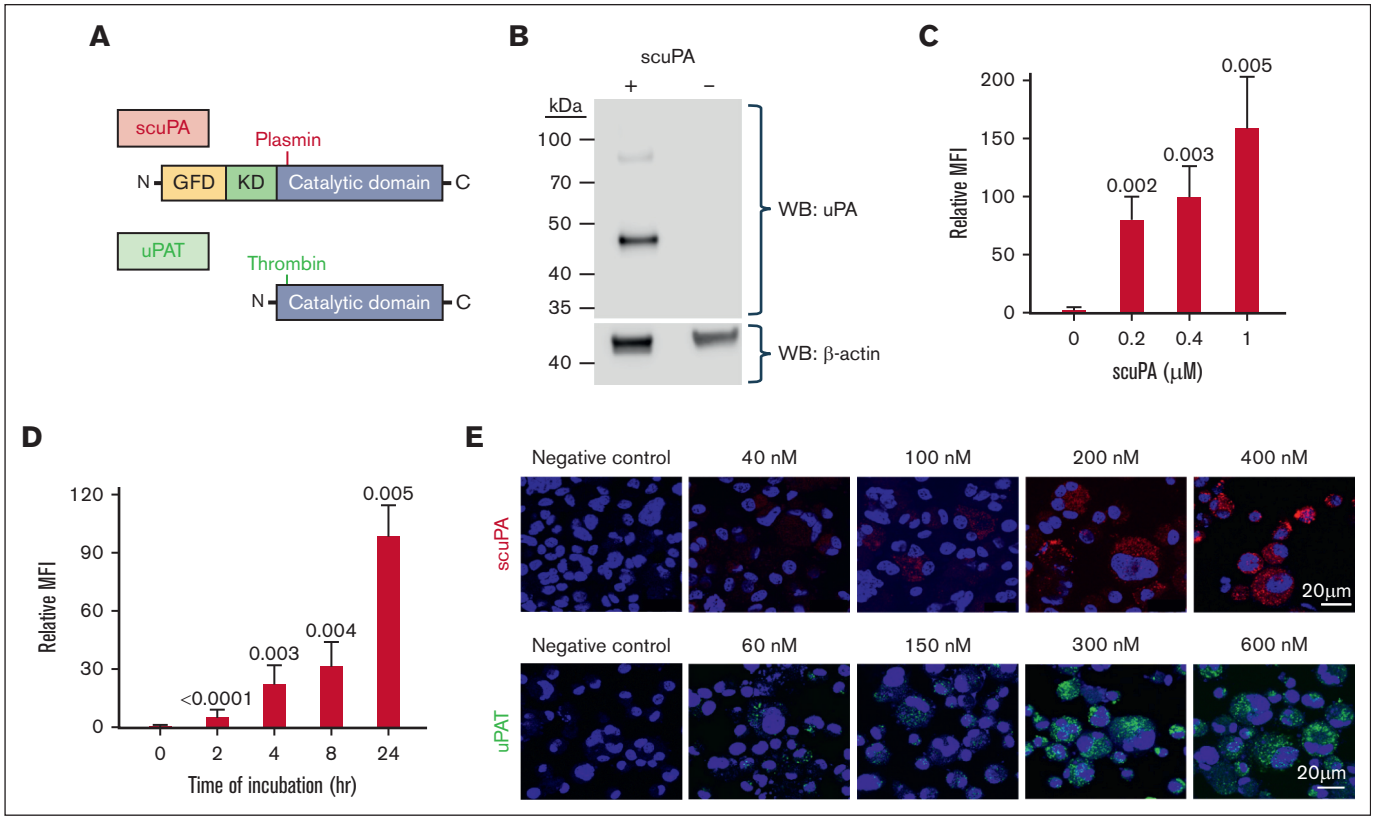

Figure 1. uPA is endocytosed by in vitro–grown MKs and stored in granules. (A) Schematics of the structures of scuPA (top) and uPAT (bottom). Full-length scuPA is composed of (1) an N-terminal growth factor-like domain (GFD, yellow) that binds uPAR; (2) a Kringle domain (K, green) that mediates LRP1-dependent intracellular uptake,[36] binding to integrins[37,38] and nuclear translocation[36]; and (3) the protease domain (catalytic domain, gray).[39] Site of activation by plasmin is shown in red. uPAT is composed of the protease domain in which $^{157}F^{158}K$ has been deleted[40] to create a thrombin cleavage/activation site (shown in green). (B) Representative WB of lysates of in vitro–grown day-11 MKs in the presence (+) or absence (–) of scuPA (400 nM) added on day 10. WB at the top was with anti-human uPA mouse monoclonal antibody followed by horseradish peroxidase (HRP)-conjugated goat anti-mouse antibody, and bottom shows HPR-conjugated anti–β-actin antibody as a loading control. Size marker is shown to the left of the blot. (C) Dose-dependent uptake of Alexa-568 scuPA by $CD34^+$ MKs. y-axes denote mean fluorescence intensity (MFI) measured by flow cytometry. Mean ± 1 standard deviation (SD) of relative uptake of scuPA compared with the values in its absence. n = 4 independent studies. P values were determined by ordinary 1-way analysis of variance (ANOVA). (D) Same as in panel C but for time course of Alexa-568 scuPA (400 nM) uptake by the $CD34^+$ MKs. (E) Visualization using confocal microscopy of Alexa-568 scuPA (top, red) or Alexa-488 uPAT (bottom, green) endocytosed by day-11 $CD34^+$ MKs for 24 hours starting on day 10 initiation of culture. DAPI (4′,6-diamidino-2-phenylindole; blue) depicts the nuclei. Scale bar is shown.

example, generated at the site of clot formation, but not by plasmin,[34] preventing uPAT activation by plasmin to avoid α-granular protein degradation seen in QPD.[35]

WB of cell lysates showed that control MKs were devoid of uPA, whereas cells incubated with scuPA showed the presence of the protein (Figure 1B). Both Alexa-568–conjugated scuPA and Alexa-488–conjugated uPAT were internalized by day-10 CD34$^+$ MKs in a concentration-dependent (Figure 1C and supplement Figure 1A, respectively) and in a time-dependent (Figure 1D and supplemental Figure 1B, respectively) manner. Both appeared as punctate particles in MKs (Figure 1E). In contrast, isolated human PLTs did not take up either uPA (supplemental Figure 2).

Pathways of uPA uptake by in vitro–generated MKs

One can suggest that scuPA and uPAT, based on their structural differences, enter MKs through different pathways and are stored in distinct granules. Alexa-568 scuPA and Alexa-488 uPAT were coincubated with CD34$^+$ MKs for 24 hours. Both scuPA and uPAT resided in the same granules as visualized by confocal microscopy, with representative data shown in Figure 2A, supplemental Figure 3, supplemental Video 1, and Table 1. To prove that the endocytosed proteins reside in the granules within the cell rather than positioned on the cell surface, we acquired serial images at different focal depths and created 3-dimensional representations to provide a composite image with a greater depth of field. Supplemental Figure 3 and supplemental Video 1 show that the endocytosed proteins reside in the same granules.

Exogenous uPA is stored in α-granules with other proteins added to the media

FV is endocytosed by human MKs and stored in α-granules.[41] To help elucidate whether uPAs endocytosed by MKs are also stored in α-granules, CD34$^+$ MKs were incubated with exogenous Alexa-488 scuPA or uPAT for 18 hours, followed by incubation with Alexa-568 FV for an additional 2 hours. By confocal microscopy, there was extensive, but not as complete, overlap as seen in Figure 2A, indicating that endocytosed scuPA or uPAT are stored in many of the same α-granules as endocytosed FV (Figure 2B and C, respectively; supplemental Figure 4; supplemental Video 2; Table 1). Furthermore, added Alexa-568 FV competed for the uptake of Alexa-488 scuPA and uPAT in in vitro–grown CD34$^+$ MKs in a concentration-dependent manner (Figure 2D and E, respectively), supporting that uPAs are stored in α-granules that contain physiologically endocytosed proteins.

Table 1. Quantification of colocalization of endocytosed or endogenous proteins in CD34$^+$ MKs via the Pearson overlap coefficient

Proteins		Pearson coefficient	N (number of cells analyzed)
A	B		
Alexa568-scuPA	Alexa488-uPAT	0.85 ± 0.03	7
Alexa488-scuPA	Alexa568-FV	0.53 ± 0.06	5
Alexa488-uPAT	Alexa568-FV	0.51 ± 0.12	5
Alexa568-scuPA	Alexa488-fibrinogen	0.70 ± 0.08	5
Alexa488-scuPA	Alexa555-FcRAP	0.65 ± 0.17	13
scuPA	IFITM-3	0.66 ± 0.11	5
scuPA	VWF	0.38 ± 0.03	7
uPAT	VWF	0.38 ± 0.03	5

uPA is taken up via LRP1

The finding that uPAT localizes within the same α-granules as scuPA and extensively colocalizes with FV led us to investigate the involvement of LRP1, which mediates FV endocytosis.[41] Prior studies showed that LRP1 is expressed during late megakaryopoiesis but is lost before PLT release,[42] and we confirmed this by WB (Figure 3A). Flow cytometry analysis also confirmed LRP1 expression on day-12 CD34$^+$ MKs (supplemental Figure 5A). Internalized scuPA is colocalized with LRP-1 in day-11 CD34$^+$ MKs (Figure 3B; supplemental Figure 6). Alexa-488 scuPA and the LRP chaperone/antagonist Alexa-555 FcRAP[27] overlapped after their endocytosis (Figure 3C; Table 1), and partially inhibited the uptake of Alexa-488 scuPA, uPAT, and FV (Figure 3D).

We asked whether PLTs released in vivo from injected MKs into NSG mice express LRP1. Nontreated and scuPA-loaded day-12 CD34$^+$ MKs were injected into NSG mice, aliquots of blood were withdrawn 6 hours after injection of MKs, and LRP1 was measured on human PLTs in whole mouse blood by flow cytometry. Like infused donor-derived PLTs, released human PLTs do not express LRP1 in the circulation whether the MKs had been exposed to scuPA or not (supplemental Figure 5B-D).

uPA and fibrinogen share an endocytic pathway in CD34$^+$ MKs

Fibrinogen is endocytosed via integrin αIIbβ3 in PLTs and MKs.[32,44] On confocal microscopy, CD34$^+$ MKs coincubated with Alexa-568 scuPA and Alexa-488 fibrinogen showed extensive overlap of the proteins (Figure 4A; supplemental Figure 7; supplemental Video 3). The αIIbβ3-blocking antibody ReoPro[28,29] reduced uptake of both fibrinogen and scuPA but did not significantly affect endocytosis of FV (Figure 4B). Coincubation with FcRAP and ReoPro did not further reduce uptake of Alexa-488 scuPA than FcRAP alone (Figure 4C), suggesting a common point in the pathway of uptake blocked by FcRAP and ReoPro. In support of this shared pathway, we observed extensive colocalization of the endocytosed scuPA, both with LRP1, which carries out endocytosis of its ligands via clathrin-coated pits[45] and with IFITM3 (Figure 4D; supplemental Figure 8; supplemental Video 4; Table 1), which mediates endocytosis of fibrinogen in CD34$^+$ MKs and PLTs through clathrin-coated pits via clathrin and αIIbβ3.[46]

Limited colocalization of uPA and endogenously expressed VWF

Next, we asked whether scuPA and/or uPAT endocytosed by CD34$^+$ MKs colocalized with endogenously expressed proteins stored in α-granules.[47] We found very limited colocalization of endocytosed scuPA and uPAT with VWF (Figure 4E; supplemental Figure 9; Table 1; supplemental Video 5) and platelet factor 4 (PF4) (supplemental Figure 10), suggesting that endocytosed uPAs and endogenous VWF are nearly completely segregated into different α-granules in MKs.

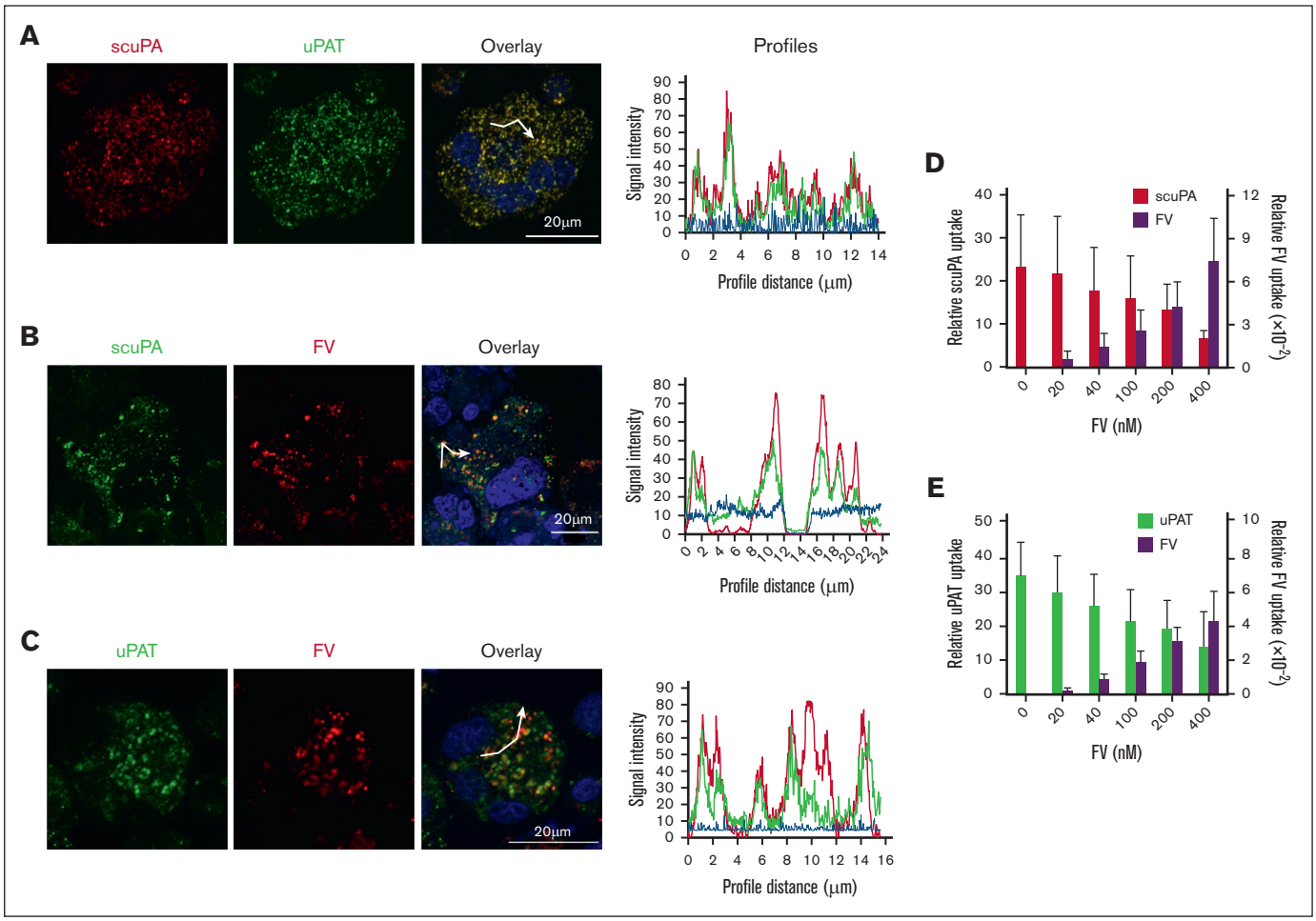

Figure 2. scuPA, uPAT, and FV share an endocytic pathway in CD34$^+$ MKs. (A) Representative confocal images of day-10 CD34$^+$ MKs loaded simultaneously by preincubation with Alexa-568 scuPA (red) and Alexa-488 uPA-T (green) for 24 hours. Nuclear staining by DAPI is in blue. Overlap is in yellow and is shown to the right. Scale bar is shown. Quantitative analysis of overlap is shown in Table 1. (B-C) Similar confocal image studies as in panel A but of CD34$^+$ MKs preincubated with (B) Alexa-488 scuPA or (C) Alexa-488 uPAT for 24 hours and then incubated with Alexa-568 FV for 2 hours (red) on day 11. White segmented lines in overlay images represent profiles along which the intensity of the fluorescence signal in each channel was measured using the ImageJ software. The plotted profiles are presented in right panels. Abscissa indicates the length of the profile in μm. Ordinate indicates relative fluorescence intensity. Coincidence of the peaks might provide clear evidence for colocalization of the signal in indicated channels. (D-E) Uptake of (D) Alexa-488 scuPA or (E) Alexa-488 uPAT, each at 400 nM, by day-11 CD34$^+$ MKs in the absence or presence of Alexa-568-FV (0-400 nM). Abscissa denotes MFI measured by flow cytometry. Mean ± 1 SD are shown. n = 4 independent experiments.

Endocytosed scuPA and uPAT differ in degradation of α-granular proteins

In QPD and in PLT uPA-transgenic mice, α-granular proteins are proteolyzed by plasmin activated by the stored uPA, potentially compromising hemostasis.[14,16-19] Therefore, we investigated whether exogenously added uPAs also trigger proteolysis of proteins stored in the α-granules of in vitro–grown CD34$^+$ MKs. Because we did not detect PLG in the lysates of in vitro–grown CD34$^+$ MKs (supplemental Figure 11), we inferred that these cells would only contain PLG in vivo if it were endocytosed from plasma. To study the effects of PLG on uPA-loaded MKs, we used CD34$^+$ MKs preloaded with Alexa-488 scuPA and Alexa-568 FV for 18 hours and then added for 18 hours Alexa-647 ncPLG, which cannot be converted to active plasmin[26] to avoid activation/degradation of endocytosed scuPA or uPAT and FV. We found significant colocalization of endocytosed uPAs, FV, and ncPLG in the α-granules of CD34$^+$ MKs (Figure 5A; supplemental Figure 12).

We asked whether endocytosed uPAs would be activated by the presence of endocytosed native PLG and lead to degradation of endocytosed FV and/or endogenous VWF. We found that the copresence of endocytosed scuPA and PLG led to degradation of FV but not VWF, on western blot (Figure 5B). A similar study, but with added uPAT instead of scuPA, resulted in less FV degradation and, again, no cleavage of endogenous VWF (Figure 5B).

In vivo studies of uPA-PLTs

Next, we examined in vivo in mice whether endocytosed uPA by in vitro–grown CD34$^+$ MKs affects thrombopoiesis and subsequent PLT half-life and agonist responsiveness. We used a model for studying the biology of released human PLTs that we had described previously (Figure 6A).[31] This model recapitulates the

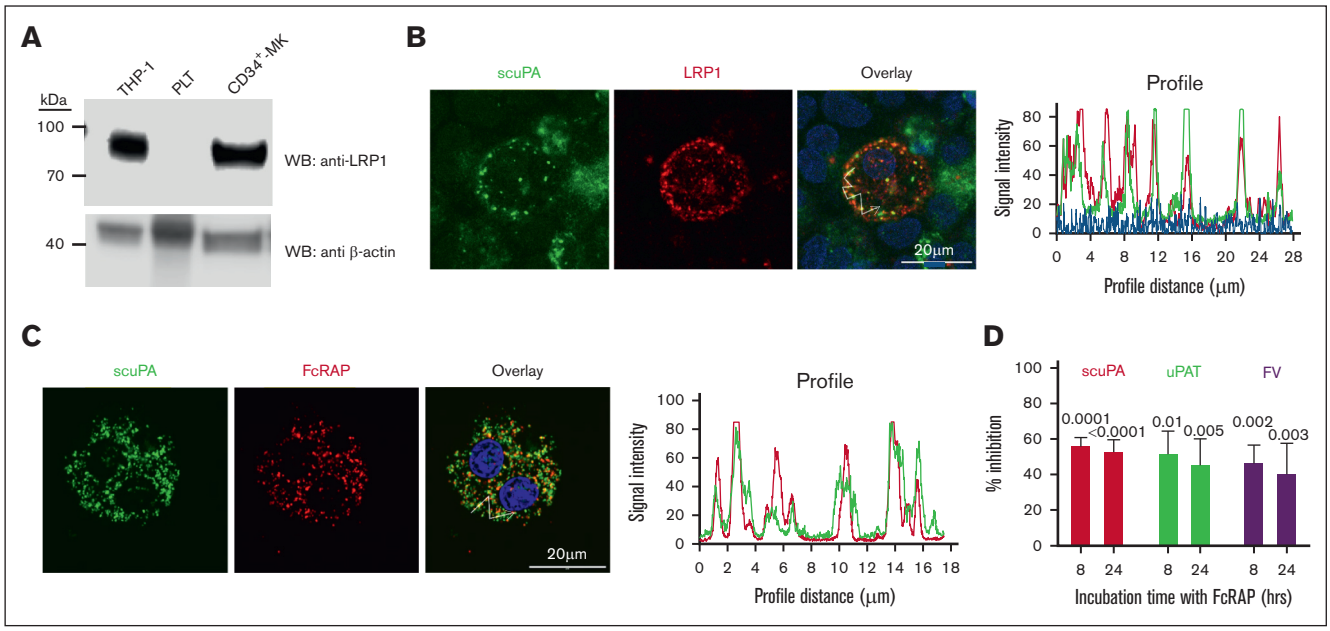

Figure 3. LRP1 mediates uptake of scuPA, uPA-T, and FV by CD34$^+$ MKs. (A) Representative WB, done as in Figure 1B, of lysates from THP-1 cell line as the positive control,[43] donor-derived PLTs, and day-11 CD34$^+$ MKs using anti-LRP light chain rabbit polyclonal antibody followed by HRP-conjugated goat anti-mouse antibody and HRP-conjugated anti–β-actin antibody as the loading control. (B) Confocal images of day-11 CD34$^+$ MKs preloaded with scuPA (1 μM) for 24 hours and stained with mouse anti-uPA monoclonal antibody and anti-LRP1 rabbit polyclonal antibody followed by Alexa-488 goat anti-mouse polyclonal antibody (green) and Alexa-555 goat anti-rabbit polyclonal antibody (red) and DAPI nuclear stain (blue). (C) Confocal images of day-11 CD34$^+$ MKs preloaded with Alexa-488 scuPA for 24 hours (green) followed by incubation with Alexa-555 FcRAP for 2 hours (red) on day 11. Scale bar is shown. Profile measurements in panels C-D are as in Figure 2A. (D) Inhibition of scuPA, uPA-T, and FV uptake by FcRAP. Day-11 CD34$^+$ MKs were incubated with Alexa-488 scuPA or Alexa-488 uPAT or Alexa-568 FV (200 nM) in the absence or presence of FcRAP (2 μM) for either 8 or 24 hours, and MFI was measured using flow cytometry. Ordinate denotes percent uptake in the presence of FcRAP relative to in its absence. Mean ± 1 SD is shown. n = 3 to 4 independent studies. Data were analyzed using an ordinary 1-way ANOVA.

pulmonary release of PLTs from MKs[48] and in which the PLTs closely resemble donor-derived PLTs.[31] We found that both unmodified and uPA-exposed MKs released a similar number of PLTs per infused MK, time to maximal PLT count, and PLT survival at 24 hours (Figure 6B). The uPA content per PLT appeared to remain stable over the study (Figure 6C) and uPA-MKs and uPA-PLTs had similar responsiveness to human-specific, thrombin receptor activating peptide 6 (Figure 6D and E, respectively).

In vivo, we also examined whether the uPA-PLTs, released from uPA-MKs, mediate thrombolysis in mice. NSG mice, which tolerate infusion of human MKs or PLTs,[31] formed carotid artery thrombi and blood flow reduction in response to Rose Bengal photochemical injury (Figure 7B, orange bar). To focus on uPA released by human PLTs, we studied NSG transgenic mice that are homozygous for a mutant murine VWF^{R1326H} that binds to the human glycoprotein Ib/IX but not mouse glycoprotein Ib/IX on PLTs. These NSG/VWF^{R1326H} mice exhibit a mild to moderate bleeding diathesis characterized by the absence of clot formation, as evidenced by greater blood flow after the photochemical injury than that of NSG mice (Figure 7B, dark grey bar vs orange bar). After injection of unmodified human CD34$^+$ MKs into NSG/VWF^{R1326H} mice, the amount of blood flow was reduced to that seen in NSG mice (Figure 7B, blue bar vs orange bar). In contrast, injection of CD34$^+$ MKs preloaded with either scuPA or uPAT, provided brisk fibrinolysis nearly to the extent seen with no human MK infusion in NSG/VWF^{R1326H} mice, consistent with the released uPA-PLTs preventing nascent thrombus formation after induction of a vascular injury (Figure 7B, red and green bars vs blue bar).[31]

We compared fibrinolysis by scuPA, packaged in MKs with nontreated MKs and with nontreated MKs plus infused scuPA (40 μg per 20 g mouse) in NSG/VWF^{R1326H} mice. Infusion of unpackaged scuPA plus nontreated MKs had a trend to increase fibrinolysis, but compared with nontreated MKs the difference was not significant (Figure 7C, pink vs orange bar), whereas fibrinolysis in mice receiving the scuPA-MKs was significantly different from the mice receiving the nontreated MKs (Figure 7C, brown vs orange bar). To estimate how much uPA is delivered into the mouse by 3×10^6 scuPA-MKs, we lysed a fixed number of scuPA-MKs and measured the concentration of uPA by enzyme-linked immunosorbent assay, and then calculated the total amount of scuPA present in 3×10^6 scuP-MKs. We calculated 8.8 ± 5.1 ng per 20 g mouse, a dose ~4500 times lower than the dose of free scuPA infused along with nontreated MKs (Figure 7C). Therefore, <10 ng scuPA packaged within MKs was ~4500 times more effective then free scuPA infused at a dose 2 mg/kg to provide similar (Figure 7C, pink vs brown bars) clot lysis effect in NSG/VWF^{R1326H} mice. These data support our hypothesis that uPA-MKs–derived uPA-PLTs release a concentrated wave of the drug locally at the nascent thrombus.

Discussion

We had pursued a promising approach to targeted thrombolysis using PLTs to deliver a fibrinolytic agent to sites of nascent

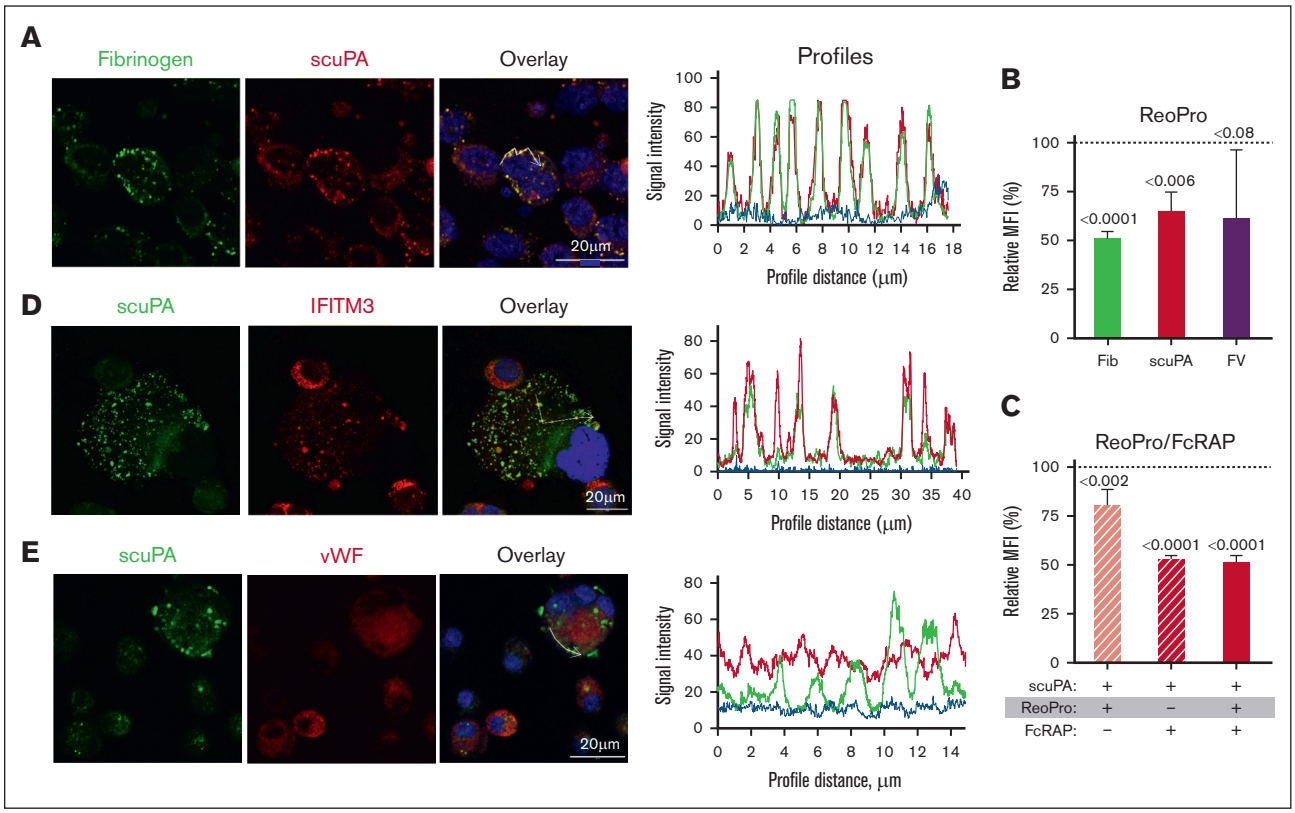

Figure 4. αIIbβ3 mediates uptake of scuPA by CD34$^+$ MKs. (A) Confocal images of day-11 CD34$^+$ MKs loaded with Alexa-488 fibrinogen and Alexa-586 scuPA for 24 hours. Colocalization of scuPA and fibrinogen is depicted in yellow in the overlay panel (right). DAPI (blue) depicts the nuclei. Scale bar is shown. For quantitation of colocalization, see also Table 1. Profile measurements are as in Figure 2A. (B) Inhibition of scuPA, fibrinogen, and FV (200 nM each) uptake by ReoPro monoclonal antibody (200 μg/mL). (C) A similar study as in panel B but for scuPA alone and inhibition was by ReoPro (200 μg/mL) and/or FcRAP (200 μg/mL). In both, ordinate denotes percent of uptake inhibition by ReoPro and/or FcRAP. Data were analyzed using the 2-way ANOVA. Mean ± 1 SD is shown. n = 3 to 4 independent studies. Data were analyzed using a 2-way Student *t* test. (D-E) Confocal studies of MKs loaded with scuPA (600 nM) and stained with Alexa-488 mouse anti-uPA monoclonal antibody, and (D) anti-IFITM3 rabbit polyclonal antibody, (E) anti-VWF antibody rabbit polyclonal antibody, followed by Alexa-555 or Alexa-647 goat anti-rabbit polyclonal antibody (red). Nuclei were stained blue by DAPI. For quantitation of overlap, see also Table 1. Profile measurements in panels D-E are as in Figure 2A.

thrombosis, avoiding lysis of mature thrombi. We called such PLTs "antithrombotic thrombocytes." Our prior in vivo studies in mice showed that infusing uPA-containing PLTs isolated from transgenic mice that expressed scuPA during megakaryopoiesis into wild-type mice led to clot lysis without causing bleeding[14]; however, it was not clear how we could translate this genetic approach to clinical care and circumvent the excessive α-granule protein proteolysis by uPA-generated plasmin, seen in QPD.[16-19] The development of technologies to generate donor-independent in vitro–generated MKs[51,52] and potentially PLTs has led to the first description of infused in vitro–generated PLTs in a patient[23] and suggested a new strategy of generating antithrombotic thrombocytes. We envisioned that in vitro–differentiated MKs could be incubated with uPA before infusion to a patient, with the released PLTs containing sufficient uPA to achieve effective fibrinolysis of incipient thrombi.

We tested 2 different uPAs: (1) scuPA being a full-length uPA that retains plasmin activation but is known to be able to be taken up by uPAR[53,54] as well as other receptor systems on MKs,[55,56] and (2) uPAT, a low–molecular weight uPA that lacks a plasmin activation site but instead can be activated by thrombin.[40] Our reason to study uPAT was to limit proteolysis of uPA in the PLT α-granule pool that is seen in QPD.[16-19] Another reason is that requiring thrombin to be present would limit proteolytic activation of uPAT to actively thrombosing sites in which thrombin would be available as opposed to mature thrombus sites.

Surprisingly, scuPA and uPAT had similar endocytic characteristics into MKs: both were targeted to the same granular pools in in vitro–differentiated MKs. Uptake of these uPAs appears to overlap with uptake of naturally endocytosed proteins, FV and fibrinogen, with considerable overlap in the granules in which they are stored. Approximately half of FV endocytosis had been reported to occur via LRP1,[41] and we show the same for the uPAs. We also show that the uPAs are also taken up via αIIbβ3 binding. Whether IFITM3, which participates in the uptake of fibrinogen in PLTs during inflammation[46] and colocalizes with endocytosed scuPA in CD34$^+$ MKs (Figure 4D), is sufficient for uPA uptake by human PLTs in inflammatory states in the absence of LRP1, or whether inflammation induces reexpression of LRP1 in PLTs enabling them to endocytose uPA, needs be elucidated in future studies. The LRP1 and αIIbβ3 pathways were not completely independent because the sum total of uptake via these 2 pathways never exceeded

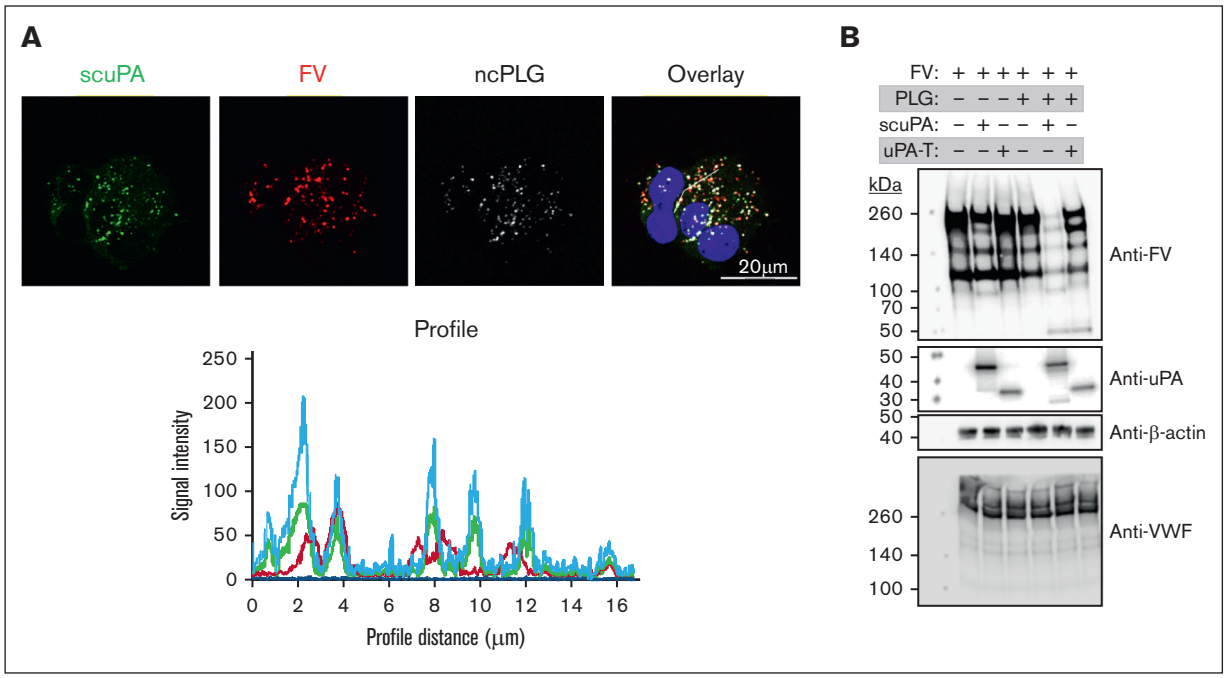

Figure 5. Effects of PLG on uPA-MKs. (A) Confocal images of day-11 CD34$^+$ MKs preincubated for 24 hours with Alexa-488 scuPA (green), Alexa-568 FV (red), and Alexa-647 ncPLG (white). Nuclei were stained blue by DAPI. For quantitation of overlap, see also Table 1. Profile measurements are as in Figure 2A. (B) WB analysis of lysates prepared from day-11 CD34$^+$ MKs with or without loading with enzymatically active PLG (20 μg/mL) on day 10 for 18 hours followed by a wash and incubation with scuPA or uPAT (200 nM each) and/or FV (400 nM) for 24 hours. WB membranes were probed with mouse monoclonal antibodies recognizing reduced FV, nonreduced uPA, and rabbit polyclonal antibody recognizing reduced VWF and β-actin (nonconjugated and HRP-conjugated, respectively).

approximately half of the total uptake of the uPAs. Whether the remaining uptake by MKs of the uPAs, FV and fibrinogen, involves a less-specific mechanism such as pinocytosis needs to be examined.[57,58]

We speculated that MKs grown in vitro in a specified cultured medium may have α-granules lacking the exogenous proteins normally endocytosed from the marrow stroma (ie, "naked α-granules") and be especially able to endocytose other proteins as part of PLT-delivered targeted therapy. Our studies showed that FV and fibrinogen added to the medium competed with uPA uptake. The highest level of uPA uptake occurred when no competing protein was present. Whether uptake was limited by α-granule storage capacity or the availability of surface receptors and their limited capacity to recycle to the surface during megakaryopoiesis is untested. What is clear is that the capacity to endocytose uPAs was lost by released PLTs, likely because of the fact that receptors, such as LRP1, were no longer present on the PLT surface (Figure 3A; supplemental Figure 2). Thus, MKs can store functionally significant amounts of a protein normally not present in these cells. The released, modified PLTs are capable of performing biological functions distinct from their natural roles.

Our studies also support that uPAT would have less risk of proteolysis of α-granular proteins than scuPA. We show that the risk is greatest for other endocytosed proteins and less so for endogenous proteins such as VWF. This is distinct from what is seen in QPD and in our transgenic mice expressing murine uPA in which both exogenous and endogenous proteins were proteolyzed.[14,35,59] We propose that PLG is initially endocytosed by MKs into an endocytosis α-granule compartment, but with time, these admixed with an endogenous α-granule compartment in the MKs and in the subsequent PLTs. Our studies with added scuPA and PLG were too short-lasting to see this admixing of the 2 original pools, and so although endocytosed FV was clearly digested, VWF in the endogenous α-granule pool was protected. In contrast to added scuPA plus PLG, added uPAT plus PLG had reduced FV proteolysis (Figure 5B).

Our murine in vivo data support that uPA-MKs retained their capacity to release functional PLTs after infusion (Figure 6). Both scuPA-PLTs and uPAT-PLTs appear to be equally effective in preventing significant thrombus growth at a site of photochemical injury in a carotid artery model. Although in the presence of added PLG, scuPA-MKs may proteolyze α-granule proteins, in the absence of added PLG to the media, scuPA as well as uPAT should not be activated, leaving all α-granule proteins intact. Whether having a thrombin-activatable site in uPAT, rather than a plasmin-activatable site in scuPA, results in more targeted fibrinolysis to the site of new thrombi and allows greater discrimination from mature thrombi need to be further tested.

Finally, besides targeted storage of uPAs in PLTs, a similar strategy of delivery of a protein of interest to a site of vascular injury has been proposed for FVIII in hemophilia A[60,61] and ADAMTS13 in thrombotic thrombocytopenic purpura.[62,63] It may also be useful to deliver antiangiogenic proteins in prevention of hematogenous cancer spread or anti-inflammatory proteins in a number of vasculitides. The further development of a practical system for in vitro–PLT preparation from MKs is the major limitation. Once

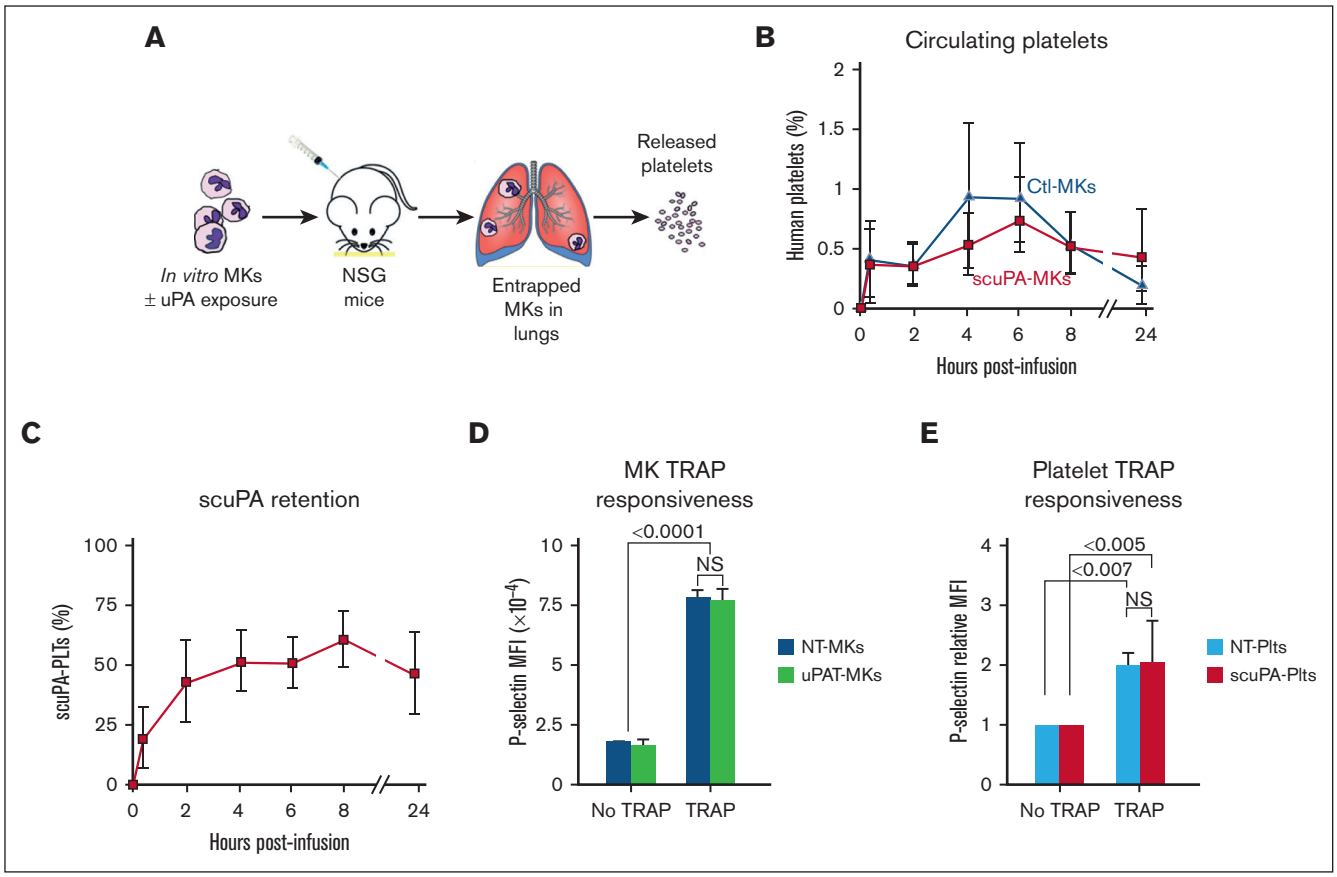

Figure 6. Release of human uPA-PLTs in vivo after infusion of not treated (NT) or scuPA-loaded CD34$^+$ MKs in NSG mice. (A) Schematic representation of intrapulmonary generation in NSG mice of human PLTs from infused CD34$^+$ MKs[49] that had or had not been incubated with exogenous uPA variant. (B) Day-12 CD34$^+$ MKs (6×10^6) that had or had not been loaded with Alexa488-scuPA (400 nM) for 24 hours were injected into NSG mice. At each time point, peripheral blood sample was withdrawn and stained with APC-human CD41 and BUV395-mouse CD41 antibodies to measure circulating human PLTs numbers relative to murine PLTs. MFI was measured using flow cytometry. Ordinate denotes percent human PLTs of the total number of human and mouse PLTs measured in the blood sample. CD34$^+$ MKs (blue) or uPA-MKs (red) infused into mice. Mean ± 1 SD is shown. n = 8 (control MKs) and n = 6 (scuPA-MKs). (C) Same experiment as in panel B but scuPA retention was determined as the percent human PLTs that remained Alexa-488 scuPA positive at indicated time points. Mean ± 1 SD is shown. n = 6. (D) Studies of agonist responsiveness for the control MKs vs uPAT-loaded MKs. Flow cytometry studies of the control MKs vs uPAT-loaded MKs at 24 hours after adding uPAT (400 nM) to the medium. P-selectin exposure after activation of the control and uPAT-loaded MKs by human-specific, thrombin receptor activating peptide 6 (TRAP6; 50 μg/mL) was measured using fluorescein isothiocyanate (FITC)-conjugated anti-human CD41 and allophycocyanin (APC)-conjugated anti–P-selectin monoclonal antibody. Mean ± 1 SD is shown. n = 3 per arm. *$P \leq .0001$ by 1-way ANOVA comparing TRAP responsiveness of NT-MKs vs uPAT-MKs. (E) Studies of agonist responsiveness for the PLTs released in vivo after infusion of NT-MKs vs scuPA-MKs. Flow cytometry studies 6 hours after infusion of the NT-MKs vs uPAT-MKs are shown. P-selectin exposure after activation of the non-treated (NT)-human (h) PLTs and uPAT-hPLTs by (TRAP6, 50 μg/mL) was measured in whole mouse blood using FITC anti-human CD41 and APC anti–P-selectin monoclonal antibody. Mean ± 1 SD is shown. n = 3 per arm. *$P \leq .0001$ by 1-way ANOVA comparing TRAP responsiveness of NT-MK–derived PLTs vs uPAT-MK–derived PLTs.

such a system is accepted clinically, its use for targeted delivery of a wide variety of therapeutics could be pursued. Many of these uses may require much smaller numbers of modified PLTs than needed for maintaining hemostasis and PLT counts.

In summary, in vitro–grown MKs in defined media can endocytose ectopic proteins such as scuPA and uPAT. The uptake of these uPAs are by pathways that overlap with those used by naturally endocytosed proteins, such as FV and fibrinogen, and the addition of these proteins can compete with uPA uptake. uPA uptake can be partially blocked by inhibiting uptake through LRP1 using FcRAP and uptake via αIIbβ3 using abciximab. These 2 overlapping pathways only account for half of uPA uptake. The basis for the remaining uptake is unclear. The endocytosed uPAs are in an α-granule pool distinct from those containing endogenously expressed proteins such as VWF and PF4. PLG is also endocytosed by MKs, and its co-uptake with scuPA and FV leads to complete FV proteolysis, but its co-uptake with uPAT leads to limited FV degradation. In these studies, VWF is not proteolyzed, consistent with their segregation to a distinct α-granule pool. In vivo studies show that thrombopoiesis and PLT biology are not affected by MK incubation with these uPAs, and the resulting PLTs can prevent nascent thrombi formation in mice. These studies suggest a new strategy for targeted intravascular therapy using in vitro–generated PLTs that may be of benefit for selective fibrinolysis and serve as a model for other potential clinical uses. However, the clinical application remains to be determined in light of the potential differences between a murine model and clinical disease, and

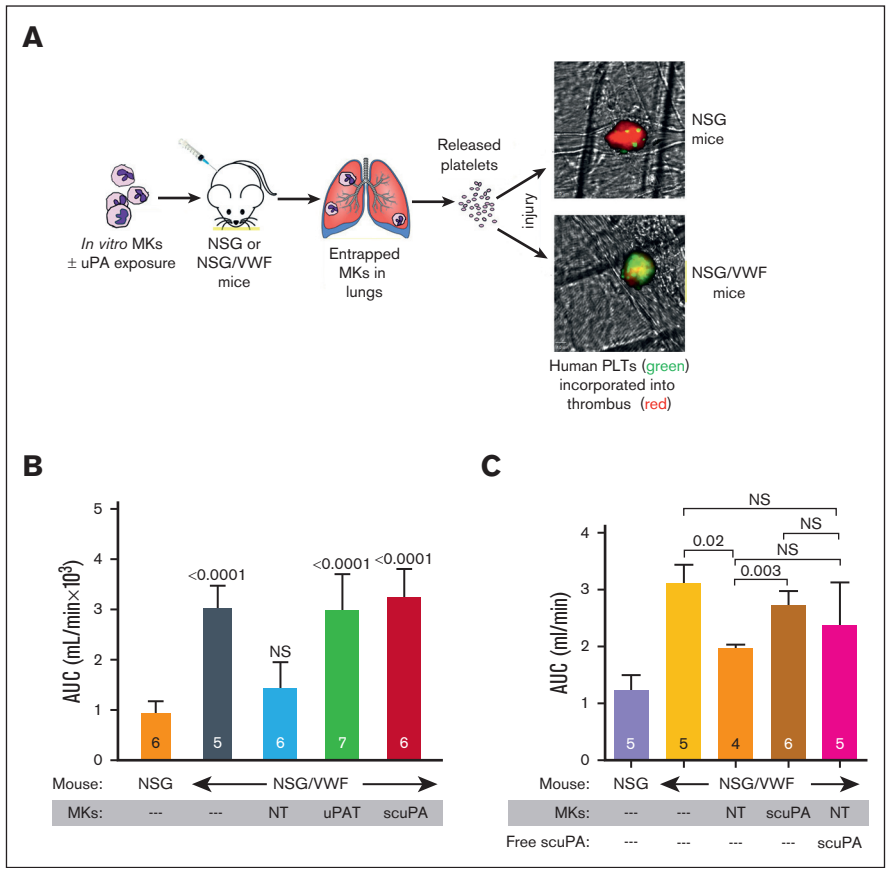

Figure 7. Antithrombotic effects of uPA-PLTs. (A) Schematic representation of the in vivo thrombosis model. Day-12 CD34$^+$ MKs that had been loaded with scuPA or uPAT for 24 hour were injected in NSG or NSG/VWF mice. Infused MKs are trapped in the lung vasculature in which they release PLTs.[49] Photochemical intravascular injury is induced by injection of Rose Bengal and exposure to a 540 nm laser.[50] Human PLT released from CD34$^+$ MKs (green) are incorporated into the nascent thrombus also containing murine PLTs (red). (B) Area under the curve (AUC) of blood flow over the first 40 minutes after injury. The genotype of the recipient mice and the infusion of CD34$^+$ MKs are shown in the abscissa as well whether the MKs had been incubated with scuPA or uPAT. The mean ± 1 SD and the number of independent experiments are shown in each bar. *P* values show outcomes in NSG/VWF studies compared with NSG control studies (orange bar) as determined by ordinary 1-way ANOVA analysis. (C) AUC of blood flow over the first 40 minutes after injury. The genotype of the recipient mice and the infusion of CD34$^+$ MKs without or along with scuPA (2 mg/kg) are shown in the abscissa as well as whether the MKs had been incubated with scuPA. The mean ± 1 SD and the number of independent experiments are shown in each bar. *P* values show outcomes in NSG/VWF studies compared with NSG control mouse (purple bar) as determined by ordinary 1-way ANOVA analysis.

because in vitro–generated MKs and PLTs are still in an early stage of clinical development.

Acknowledgments

The authors thank the University of Pennsylvania Cell & Developmental Biology Microscopy Core for management of confocal microscopy experiments, and the CHOP Flow Facility Core for management of flow cytometry experiments.

Support for this study came from the following National Institutes of Health (NHLBI) grants: R35 HL150698 (M.P.), RO1HL141462 (V.S.), RO1HL159256 (D.B.C.), and P01 HL139420, Project 2 (R.M.C.), and Russian Science Foundation grant 23-15-00540 (K.V.D.).

Authorship

Contribution: M.P. along with V.S. provided overall leadership and experimental design and manuscript preparation; S.V.Z. prepared and characterized uPAs and performed the confocal and western blot studies; H.A. carried out the cell growth studies and the flow cytometric and in vivo studies; S.V.Z. and H.A. contributed to the data analysis and writing; M.A.K., K.B., K.V.D., L.I., and R.M.C. contributed important ingredients for these studies; and D.B.C. made valuable insights to the studies and their interpretation, and to manuscript preparation.

Conflict-of-interest disclosure: The authors declare no competing financial interests.

ORCID profiles: M.P., 0000-0001-7237-3613; L.I., 0000-0003-3468-8600; R.M.C., 0000-0002-0585-4537; D.B.C., 0000-0001-5986-504X.

Correspondence: Victoria Stepanova, Department of Pathology and Laboratory Medicine, University of Pennsylvania Perelman School of Medicine, 513B Stellar Chance Bld, 422 Curie Blvd, Philadelphia, PA 19104; email: vstepano@pennmedicine.upenn.edu.

References

1. Abdul Rahim P, Rengaswamy D. Fibrinolytic enzyme - an overview. *Curr Pharm Biotechnol*. 2022;23(11):1336-1345.
2. Altaf F, Wu S, Kasim V. Role of fibrinolytic enzymes in anti-thrombosis therapy. *Front Mol Biosci*. 2021;8:680397.
3. Risman RA, Kirby NC, Bannish BE, Hudson NE, Tutwiler V. Fibrinolysis: an illustrated review. *Res Pract Thromb Haemost*. 2023;7(2):100081.
4. Tang M, Hu C, Lin H, Yan H. Fibrinolytic drugs induced hemorrhage: mechanisms and solutions. *Blood Coagul Fibrinolysis*. 2023;34(5):263-271.

5. Kaufman C, Kinney T, Quencer K. Practice trends of fibrinogen monitoring in thrombolysis. *J Clin Med*. 2018;7(5):111.
6. Modi NB, Fox NL, Clow FW, et al. Pharmacokinetics and pharmacodynamics of tenecteplase: results from a phase II study in patients with acute myocardial infarction. *J Clin Pharmacol*. 2000;40(5):508-515.
7. Medcalf RL. Fibrinolysis: from blood to the brain. *J Thromb Haemost*. 2017;15(11):2089-2098.
8. Marshall PS, Mathews KS, Siegel MD. Diagnosis and management of life-threatening pulmonary embolism. *J Intensive Care Med*. 2011;26(5):275-294.
9. Clever YP, Cremers B, Link A, Bohm M, Scheller B. Long-term follow-up of early versus delayed invasive approach after fibrinolysis in acute myocardial infarction. *Circ Cardiovasc Interv*. 2011;4(4):342-348.
10. Thiele H, Eitel I, Meinberg C, et al. Randomized comparison of pre-hospital-initiated facilitated percutaneous coronary intervention versus primary percutaneous coronary intervention in acute myocardial infarction very early after symptom onset: the LIPSIA-STEMI trial (Leipzig immediate prehospital facilitated angioplasty in ST-segment myocardial infarction). *JACC Cardiovasc Interv*. 2011;4(6):605-614.
11. Fuentes RE, Zaitsev S, Ahn HS, et al. A chimeric platelet-targeted urokinase prodrug selectively blocks new thrombus formation. *J Clin Invest*. 2016;126(2):483-494.
12. Zaitsev S, Spitzer D, Murciano JC, et al. Sustained thromboprophylaxis mediated by an RBC-targeted pro-urokinase zymogen activated at the site of clot formation. *Blood*. 2010;115(25):5241-5248.
13. Byrnes JR, Wolberg AS. Red blood cells in thrombosis. *Blood*. 2017;130(16):1795-1799.
14. Kufrin D, Eslin DE, Bdeir K, et al. Antithrombotic thrombocytes: ectopic expression of urokinase-type plasminogen activator in platelets. *Blood*. 2003;102(3):926-933.
15. Wu G, Mazzitelli BA, Quek AJ, et al. Tranexamic acid is an active site inhibitor of urokinase plasminogen activator. *Blood Adv*. 2019;3(5):729-733.
16. Blavignac J, Bunimov N, Rivard GE, Hayward CP. Quebec platelet disorder: update on pathogenesis, diagnosis, and treatment. *Semin Thromb Hemost*. 2011;37(6):713-720.
17. Diamandis M, Paterson AD, Rommens JM, et al. Quebec platelet disorder is linked to the urokinase plasminogen activator gene (PLAU) and increases expression of the linked allele in megakaryocytes. *Blood*. 2009;113(7):1543-1546.
18. Hayward CP, Liang M, Tasneem S, et al. The duplication mutation of Quebec platelet disorder dysregulates PLAU, but not C10orf55, selectively increasing production of normal PLAU transcripts by megakaryocytes but not granulocytes. *PLoS One*. 2017;12(3):e0173991.
19. Lee D, Walega DR. Management of Quebec platelet disorder for cervical facet injections in the outpatient setting: a case report. *In Pract*. 2020;14(6):e01187.
20. Matsunaga T, Tanaka I, Kobune M, et al. Ex vivo large-scale generation of human platelets from cord blood CD34+ cells. *Stem Cell*. 2006;24(12):2877-2887.
21. Matsubara Y, Saito E, Suzuki H, Watanabe N, Murata M, Ikeda Y. Generation of megakaryocytes and platelets from human subcutaneous adipose tissues. *Biochem Biophys Res Commun*. 2009;378(4):716-720.
22. Sullivan SK, Mills JA, Koukouritaki SB, et al. High-level transgene expression in induced pluripotent stem cell-derived megakaryocytes: correction of Glanzmann thrombasthenia. *Blood*. 2014;123(5):753-757.
23. Sugimoto N, Kanda J, Nakamura S, et al. iPLAT1: the first-in-human clinical trial of iPSC-derived platelets as a phase 1 autologous transfusion study. *Blood*. 2022;140(22):2398-2402.
24. Zhang N, Newman PJ. Packaging functionally important plasma proteins into the α-granules of human-induced pluripotent stem cell-derived megakaryocytes. *J Tissue Eng Regen Med*. 2019;13(2):244-252.
25. Jarocha D, Vo KK, Lyde RB, Hayes V, Camire RM, Poncz M. Enhancing functional platelet release in vivo from in vitro-grown megakaryocytes using small molecule inhibitors. *Blood Adv*. 2018;2(6):597-606.
26. Higazi AA, Ajawi F, Akkawi S, Hess E, Kuo A, Cines DB. Regulation of the single-chain urokinase-urokinase receptor complex activity by plasminogen and fibrin: novel mechanism of fibrin specificity. *Blood*. 2005;105(3):1021-1028.
27. Makarova AM, Lebedeva TV, Nassar T, et al. Urokinase-type plasminogen activator (uPA) induces pulmonary microvascular endothelial permeability through low density lipoprotein receptor-related protein (LRP)-dependent activation of endothelial nitric-oxide synthase. *J Biol Chem*. 2011;286(26):23044-23053.
28. Coller BS, Anderson K, Weisman HF. New antiplatelet agents: platelet GPIIb/IIIa antagonists. *Thromb Haemost*. 1995;74(1):302-308.
29. Tcheng JE, Kereiakes DJ, Lincoff AM, et al. Abciximab readminstration: results of the ReoPro Readministration Registry. *Circulation*. 2001;104(8):870-875.
30. Adair BD, Alonso JL, van Agthoven J, et al. Structure-guided design of pure orthosteric inhibitors of alphaIIbbeta3 that prevent thrombosis but preserve hemostasis. *Nat Commun*. 2020;11(1):398.
31. Lee K, Ahn HS, Estevez B, Poncz M. RUNX1-deficient human megakaryocytes demonstrate thrombopoietic and platelet half-life and functional defects. *Blood*. 2023;141(3):260-270.
32. Harrison P, Wilbourn B, Debili N, et al. Uptake of plasma fibrinogen into the alpha granules of human megakaryocytes and platelets. *J Clin Invest*. 1989;84(4):1320-1324.
33. Tkaczynski J, Lyde RB, Ahn H, et al. A novel approach for generating platelet-delivered FVIII: role of transient LRP1 expression during megakaryopoiesis. *Blood*. 2019;134(suppl 1):1102.

34. Conese M, Blasi F. Urokinase/urokinase receptor system: internalization/degradation of urokinase-serpin complexes: mechanism and regulation. *Biol Chem Hoppe Seyler*. 1995;376(3):143-155.
35. Diamandis M, Veljkovic DK, Maurer-Spurej E, Rivard GE, Hayward CP. Quebec platelet disorder: features, pathogenesis and treatment. *Blood Coagul Fibrinolysis*. 2008;19(2):109-119.
36. Stepanova V, Lebedeva T, Kuo A, et al. Nuclear translocation of urokinase-type plasminogen activator. *Blood*. 2008;112(1):100-110.
37. Kwak SH, Mitra S, Bdeir K, et al. The kringle domain of urokinase-type plasminogen activator potentiates LPS-induced neutrophil activation through interaction with {alpha}V{beta}3 integrins. *J Leukoc Biol*. 2005;78(4):937-945.
38. Tarui T, Akakura N, Majumdar M, et al. Direct interaction of the kringle domain of urokinase-type plasminogen activator (uPA) and integrin alpha v beta 3 induces signal transduction and enhances plasminogen activation. *Thromb Haemost*. 2006;95(3):524-534.
39. Orgel D, Schroder W, Hecker-Kia A, Weithmann KU, Kolkenbrock H, Ulbrich N. The cleavage of pro-urokinase type plasminogen activator by stromelysin-1. *Clin Chem Lab Med*. 1998;36(9):697-702.
40. Ding BS, Hong N, Murciano JC, et al. Prophylactic thrombolysis by thrombin-activated latent prourokinase targeted to PECAM-1 in the pulmonary vasculature. *Blood*. 2008;111(4):1999-2006.
41. Bouchard BA, Meisler NT, Nesheim ME, Liu CX, Strickland DK, Tracy PB. A unique function for LRP-1: a component of a two-receptor system mediating specific endocytosis of plasma-derived factor V by megakaryocytes. *J Thromb Haemost*. 2008;6(4):638-644.
42. Lambert MP, Wang Y, Bdeir KH, Nguyen Y, Kowalska MA, Poncz M. Platelet factor 4 regulates megakaryopoiesis through low-density lipoprotein receptor-related protein 1 (LRP1) on megakaryocytes. *Blood*. 2009;114(11):2290-2298.
43. Deng N, Li M, Shen D, et al. LRP1 receptor-mediated immunosuppression of alpha-MMC on monocytes. *Int Immunopharmacol*. 2019;70:80-87.
44. Handagama P, Scarborough RM, Shuman MA, Bainton DF. Endocytosis of fibrinogen into megakaryocyte and platelet alpha-granules is mediated by alpha IIb beta 3 (glycoprotein IIb-IIIa). *Blood*. 1993;82(1):135-138.
45. Czekay RP, Kuemmel TA, Orlando RA, Farquhar MG. Direct binding of occupied urokinase receptor (uPAR) to LDL receptor-related protein is required for endocytosis of uPAR and regulation of cell surface urokinase activity. *Mol Biol Cell*. 2001;12(5):1467-1479.
46. Campbell RA, Manne BK, Banerjee M, et al. IFITM3 regulates fibrinogen endocytosis and platelet reactivity in nonviral sepsis. *J Clin Invest*. 2022;132(23):e153014.
47. Nurden P, Debili N, Vainchenker W, et al. Impaired megakaryocytopoiesis in type 2B von Willebrand disease with severe thrombocytopenia. *Blood*. 2006;108(8):2587-2595.
48. Zhao X, Alibhai D, Walsh TG, et al. Highly efficient platelet generation in lung vasculature reproduced by microfluidics. *Nat Commun*. 2023;14(1):4026.
49. Wang Y, Hayes V, Jarocha D, et al. Comparative analysis of human ex vivo-generated platelets vs megakaryocyte-generated platelets in mice: a cautionary tale. *Blood*. 2015;125(23):3627-3636.
50. Rauova L, Hirsch JD, Greene TK, et al. Monocyte-bound PF4 in the pathogenesis of heparin-induced thrombocytopenia. *Blood*. 2010;116(23):5021-5031.
51. Sugimoto N, Nakamura S, Shimizu S, et al. Production and nonclinical evaluation of an autologous iPSC-derived platelet product for the iPLAT1 clinical trial. *Blood Adv*. 2022;6(23):6056-6069.
52. Nakamura S, Takayama N, Hirata S, et al. Expandable megakaryocyte cell lines enable clinically applicable generation of platelets from human induced pluripotent stem cells. *Cell Stem Cell*. 2014;14(4):535-548.
53. Blasi F. The urokinase receptor in hematopoietic stem cells mobilization. *Curr Pharm Des*. 2011;17(19):1911-1913.
54. Roldan AL, Cubellis MV, Masucci MT, et al. Cloning and expression of the receptor for human urokinase plasminogen activator, a central molecule in cell surface, plasmin dependent proteolysis. *EMBO J*. 1990;9(2):467-474.
55. Nassar T, Yarovoi S, Fanne RA, et al. Regulation of airway contractility by plasminogen activators through N-methyl-D-aspartate receptor-1. *Am J Respir Cell Mol Biol*. 2010;43(6):703-711.
56. Nassar T, Yarovoi S, Fanne RA, et al. Urokinase plasminogen activator regulates pulmonary arterial contractility and vascular permeability in mice. *Am J Respir Cell Mol Biol*. 2011;45(5):1015-1021.
57. Zhao H, Gulesserian S, Ganesan SK, et al. Inhibition of megakaryocyte differentiation by antibody-drug conjugates (ADCs) is mediated by macropinocytosis: implications for ADC-induced thrombocytopenia. *Mol Cancer Ther*. 2017;16(9):1877-1886.
58. Bauer A, Frascaroli G, Walther P. Megapinosomes and homologous structures in hematopoietic cells. *Histochem Cell Biol*. 2022;158(3):253-260.
59. Diamandis M, Adam F, Kahr WH, et al. Insights into abnormal hemostasis in the Quebec platelet disorder from analyses of clot lysis. *J Thromb Haemost*. 2006;4(5):1086-1094.
60. Lyde RB, Ahn HS, Vo KK, et al. Infused factor VIII-expressing platelets or megakaryocytes as a novel therapeutic strategy for hemophilia A. *Blood Adv*. 2019;3(9):1368-1378.
61. Yarovoi HV, Kufrin D, Eslin DE, et al. Factor VIII ectopically expressed in platelets: efficacy in hemophilia A treatment. *Blood*. 2003;102(12):4006-4013.
62. Pickens B, Mao Y, Li D, et al. Platelet-delivered ADAMTS13 inhibits arterial thrombosis and prevents thrombotic thrombocytopenic purpura in murine models. *Blood*. 2015;125(21):3326-3334.
63. Abdelgawwad MS, Cao W, Zheng L, Kocher NK, Williams LA, Zheng XL. Transfusion of platelets loaded with recombinant ADAMTS13 (a disintegrin and metalloprotease with thrombospondin type 1 repeats-13) is efficacious for inhibiting arterial thrombosis associated with thrombotic thrombocytopenic purpura. *Arterioscler Thromb Vasc Biol*. 2018;38(11):2731-2743.